Zhou Xuhui (Orcid ID: 0000-0002-2038-9901)
McDowell Nathan (Orcid ID: 0000-0002-2178-2254)

Embolism resistance explains mortality and recovery of five subtropical evergreen broadleaf trees to persistent drought

Junjiong Shao[1,2], Xuhui Zhou[1,3*], Peipei Zhang[1,4], Deping Zhai[1,5], Tengfei Yuan[1,6], Zhen Li[1], Yanghui He[1,3], Nate G. McDowell[7,8]

[1]*Center for Global Change and Ecological Forecasting, Tiantong National Field Observation Station for Forest Ecosystem, School of Ecological and Environmental Sciences, East China Normal University, Shanghai, 200241, China*

[2]*State Key Laboratory of Subtropical Silviculture, Zhejiang A&F University, Hangzhou, 311300, China*

[3]*Northeast Asia ecosystem Carbon sink research Center (NACC), Center for Ecological Research, Key Laboratory of Sustainable Forest Ecosystem Management-Ministry of Education, School of Forestry, Northeast Forestry University, Harbin 150040, China.*

[4]*CAS Key Laboratory of Mountain Ecological Restoration and Bioresource Utilization & Ecological Restoration and Biodiversity Conservation Key Laboratory of Sichuan Province, Chengdu Institute of Biology, Chinese Academy of Sciences, Chengdu, 610041, China*

[5]*School of Ecology and Environmental Science, Yunnan University, Kunming, 650091, China*

[6]*School of Atmospheric Sciences, Nanjing University, Nanjing, 210023, China*

[7]*Atmospheric Sciences and Global Change Division, Pacific Northwest National Lab, PO Box 999, Richland, WA, 99352*

[8]*School of Biological Sciences, Washington State University, PO Box 644236, Pullman, WA 99164-4236*

Corresponding Author: Xuhui Zhou. E-mail: xhzhou@des.ecnu.edu.cn

Open Research Statement: Data (Shao, 2022) is archived at Figshare at https://doi.org/10.6084/m9.figshare.20326380.v1

Abstract

Subtropical evergreen broadleaf forest (SEBF) is experiencing and expected to suffer more frequent and severe drought events. However, how the hydraulic traits directly link to the mortality and recovery of SEBF trees remains unclear. In this study, we conducted a drought-rewatering experiment on tree seedlings of five dominant species to investigate how the hydraulic traits were related to tree mortality and the resistance and recovery of photosynthesis (A) and transpiration (E) under different drought severities. Species with greater embolism resistance (P_{50}) survived longer than those with the weaker P_{50}. However, there was no general hydraulic threshold associated with tree mortality, with the lethal hydraulic failure varying from 64% to 93% loss of conductance. The photosynthesis and transpiration of tree species with greater P_{50} were more resistant to and recovered faster from drought than those with lower P_{50}. Other plant traits could not explain the interspecific variation in tree mortality and drought resistance and recovery. These results highlight the unique importance of embolism resistance in driving carbon and water process under persistent drought across different trees in SEBF. The absence of multiple efficient drought strategies in SEBF seedlings implies the difficulty of natural seedling regeneration under future droughts, which often occurs after destructive disturbances (e.g., extreme drought events and typhoon), suggesting that this biome may be highly vulnerable to co-ocurring climate extremes.

Keywords: drought-rewatering, embolism resistance, PLC threshold, recovery, subtropical forest, tree mortality

1 INTRODUCTION

Forest ecosystems are critical to global biodiversity and the carbon sink (Pan *et al.*, 2013). However, in the context of climate change, more frequent and severe drought events have induced substantial forest mortality and hampered ecosystem functions (Hartmann *et al.*, 2018; McDowell *et al.*, 2022). As two paramount functions, the carbon and water dynamics are key processes mediating the feedbacks between forests and the climate system (Haughton *et al.*, 2018). Unfortunately, forecasting the carbon and water fluxes under drought suffers great uncertainty (Vargas *et al.*, 2013), largely due to the insufficient understanding on the resilience of tree physiological processes (e.g., photosynthesis and transpiration).

Two measurable components of 'resilience' are 'resistance' and 'recovery', which quantify the impact of an exogenous disturbance on a system and the rate and magnitude of recovery, respectively (Hodgson *et al.*, 2015). Previous studies showed that species-level differences in resistance to drought (Roman *et al.*, 2015; Anderegg *et al.*, 2016) could be attributed to differences in hydraulic processes. For example, photosynthesis (A) and transpiration (E) of relatively isohydric plants (i.e., small declines in mid-day water potential despite drying soil) may be highly sensitive to drought because they closed stomata more rapidly than relatively anisohydric plants (Martinez-Vilalta *et al.*, 2014). In contrast, species with higher embolism resistance or deeper rooting depths are able to maintain higher water potential and hydraulic conductance, suggesting that their physiological rates (e.g., A and E) are more resistant to severe drought (Meinzer & McCulloh, 2013). In addition, plants with greater turgor loss point (π_{tlp}) in leaves were more tolerant to internal water limitations, thus buffering stomata closure (Zhu *et al.*, 2018). These hydraulic characteristics may be coordinated with each other, and correlated with other functional traits, as a result of co-selections on plant traits (Bartlett *et al.*, 2016; Mursinna *et al.*, 2018). However, there are also studies showing decoupling between them (L. Li *et al.*, 2015; Kannenberg *et al.*, 2019), which raises the question whether multiple plant traits would co-regulate the drought resistance in forests.

The extreme impact of drought on tree physiology may ultimately trigger death (McDowell *et al.*, 2013). A tipping point of hydraulic failure may occur after trees die (Urli *et al.*, 2013; Hammond *et al.*, 2019). However, the exact extent of hydraulic failure inducing tree mortality varies among studies, with values from 50 percentage loss of stem conductance (PLC) to > 80% PLC (Kursar *et al.*, 2009; Brodribb *et al.*, 2010; McDowell *et al.*, 2013; Urli *et al.*, 2013; Hammond *et al.*, 2019). This large variation of lethal stem PLC might reflect the complicated mechanisms with two questions: whether trees can recover through embolism refilling or new xylem growth after drought (Gauthey *et al.*, 2022), and whether the hydraulic systems in leaf and root are more vulnerable to drought than that in stem (Creek *et al.*, 2018; Levionnois *et al.*, 2020). Although the concept of a point of no return of hydraulic failure has been widely adopted, a common value of PLC causing tree death is not apparent.

Compared to research on drought resistance and mortality, those focusing on the role of plant traits in regulating post-drought recovery are relatively rare, and the conclusions are more uncertain. Among a few studies, some showed that higher level of xylem embolism limited post-drought recovery (Urli *et al.*, 2013; Peguero-Pina *et al.*, 2018), whereas others suggested that plants with lower embolism resistance may have higher ability to repair the embolism (Klein *et al.*, 2018). Similarly, on one hand, relatively isohydric plants might showed more rapid post-drought recovery of photosynthesis than anisohydric plants due to the lower risk of hydraulic failure (Kannenberg *et al.*, 2019). On the other hand, isohydric plants could also exhibit slow post-drought recovery (Garcia-Forner *et al.*, 2016) because they have lower photosynthate, which provides energy for signaling of stomatal response, osmotic adjustments, and embolism refilling, than anisohydric plants under drought stress (Pou *et al.*, 2012; Klein *et al.*, 2018). Therefore, whether a particular trait would regulate the recovery of photosynthesis and transpiration needs to be confirmed by experiments designed to investigate the resilience of tree physiology.

Subtropical evergreen broadleaf forests (SEBFs), which have a large distribution in southern China, are a global hotspot for biodiversity and carbon sequestration (Yu *et al.*, 2014; Fan *et al.*, 2018). Historical observations and model forecasting suggest that southern China has suffered and will experience more severe, frequent, and extensive droughts (Dai, 2013; Yuan *et al.*, 2016). Historically, the selection pressure induced by water deficit in SEBFs is not as strong as that in arid ecosystems. Therefore, the mechanisms underlying the drought resistance and resilience of SEBF species may be different from those underlying the species grown in arid biomes such as Mediterranean forests or arid grasslands.

To explore the mechanisms driving interspecific differences in drought resistance and resilience among SEBF species, we performed a common garden drought-rewatering experiment on seedlings of five dominant species with differential drought sensitivities at a SEBF in China. A drought gradient was created by withholding water for different number of days (8, 14, 20, 26, 32, 38 and 44 days, respectively). To understand recovery dynamics, a subset of plants was rewatered for each level of drought gradient after the corresponding number of days of water withholding. Plant morphological, photosynthetic, and hydraulic traits were examined in relation to the response and recovery of photosynthesis and transpiration. Our main objectives were: (1) to explore which plant traits explained the interspecific differences in tree mortality and drought resistance and recovery, and (2) to investigate whether a general PLC threshold for tree death exists among the studied trees.

2 METHODS

2.1 Study site and experimental design

The experiment was carried out in a common garden located in Ningbo, Zhejiang Province, China (29.86°N, 121.34°E). This region is characterized by hot-wet summer and cool-dry winter. The mean annual temperature and precipitation was 16.2 ºC and 1374 mm, respectively. Precipitation occurs primarily from May to August, but there are heat weaves and extreme droughts during this period in some years. In 2017, there was no rainfall during the entire August, resulting in an extremely dry summer. The natural vegetation is subtropical evergreen broadleaf forest, with a growing season from May to October. Soils were mainly red or yellow earths with high abundance of iron and aluminium oxides as an Acrisol soil. The substrate of parental material was mesozoic sediments and acidic intrusive rocks. Soil pH was 4.4 - 5.1, and texture was a clay loam (6.8% sand, 55.5% silt, and 4.7% clay; Yan *et al.*, 2006).

Five dominant tree species were selected (*Cyclobalanopsis gilva*, *Castanopsis sclerophylla*, *Neocinnamomum chekiangense*, *Phoebe chekiangensis* and *Schima superba*). According to previous observations, *C. sclerophylla* and *S. superba* were relatively insensitive, whereas *P. chekiangensis* was highly sensitive to water deficit (Duan *et al.*, 2019; Li *et al.*, 2019). Overall, these species represented a wide range of drought sensitivities in the studied forest.

A total of 1250 (250 for each species) two- to three-year-old seedlings were transplanted from a nursery garden into 18L plastic pots (30 cm diameter and 25 cm height) during 10-15 April, 2017. The substrate was yellow soil with 5.6% peat, 2.0% manure, and 1.0% calcium superphosphate. The pots were located in the field with full irrigation for three months. On 10 July, all pots were transferred into a greenhouse covered with transparent plastic film (90% transmittance) on top but with the surrounding walls open to the atmosphere, allowing thorough cross-ventilation. The plants were fully irrigated for two weeks to allow maximum acclimation to their new environment. Drought treatments began on 26 July (DOY 206). For each species, there were one control group with sufficient water and seven drought-rewatering groups with water being withheld for 8, 14, 20, 26, 32, 38 and 44 days, respectively. After each group reached its required days of drought, the plants were fully irrigated until the end of September (DOY 273). However, the measurements stopped once the trees fully recovered, died or had no signs of further recover after 30 days of rewetting. For the plants partially recovered, it was the end of growing season after 30 days of rewetting, in which period the plants did not develop new leaves. These plants may fully recover in the spring of next year, but it is beyond our scope. The measurements of physiological parameters and biomass during soil drying and recovery processes were conducted on three replications, whereas the measurements of plant traits were conducted on varied replications (see Table 1 for details).

2.2 Measurements of environmental variables

To continuously trace the temperature and relative humidity in the greenhouse, two hygrothermographs were located at 1.8 m height. Two methods were used to monitor soil water content (SWC). One was the weighing method timed when there weas destructive samplings. In detail, soils at 10 cm depth were sampled and put in aluminium boxes for oven-drying at 105 °C for 24 hours. The soil weights before and after oven-drying were used to calculate SWC. The other method was a portable soil moisture meter that measures SWC non-destructivly. In order to account for the systematic difference, SWC from the second method was corrected by using the linear relationship between the two methods. The relationship was $y = 1.02x – 0.35$, ($r^2 = 0.67$, $P < 0.001$).

2.3 Measurements of plant traits

2.3.1 Morphological traits

Morphological traits included plant height, basal diameter, leaf size, specific leaf area (SLA), leaf dry matter content (LDMC), leaf area:basal area ratio, wood density and root:shoot biomass ratio. These measurements generally followed the handbook of Pérez-Harguindeguy *et al.* (2013). Specifically, plant height and stem diameter were measured on all plants. Leaf area:basal area ratio, woody density and root:shoot ratio were measured on five randomly selected individuals for each species. Leaf size, SLA and LDMC were measured on five individuals with five mature leaves for each individual. These measurements were conducted before the drought treatment during 20 – 26 July.

2.3.2 Photosynthetic traits

Photosynthetic traits, including the parameters of light and CO_2 response curves of five individuals, were collected before the drought treatment using a portable photosynthesis apparatus (LI-6400; LI-COR) from 8:00-11:00 on sunny days. The light response curves were measured at ambient CO_2 concentration, with the temperature and relative humidity in the chamber being around 25 °C and 60%, respectively. The light intensity gradient was 1500, 1000, 500, 250, 120, 60, 40, 20, 10 and 0 μ mol m^{-2} s^{-1}. For the CO_2 response curves, the temperature, relative humidity and light intensity in the chamber were maintained at 25 °C, 60% and 1000 μ mol m^{-2} s^{-1}, respectively. The CO_2 gradient was 400, 50, 100, 150, 200, 250, 350, 500, 700, 900, 1200 and 1400 ppm. The light response curve was fitted by the Michaelis-Menten model (de A. Lobo *et al.*, 2013). Light saturated photosynthesis (A_{m}), Michaelis constant (K_{m}), dark respiration (R_{d}), light compensation point (*LCP*), and apparent quantum yield (α, ratio of A_{m} to K_{m}) were calculated. The CO_2 response curve was fitted by the FvCB model (Duursma, 2015):

$$A_{\mathrm{m}} = \frac{A_{\mathrm{c}} + A_{\mathrm{j}} - \sqrt{\left(A_{\mathrm{c}} + A_{\mathrm{j}}\right)^2 - 4\theta A_{\mathrm{c}} A_{\mathrm{j}}}}{2\theta} - R_{\mathrm{d}} \tag{1}$$

$$A_{\mathrm{c}} = \frac{V_{\mathrm{cmax}}(C_i - \Gamma^*)}{\left[C_{\mathrm{i}} + K_{\mathrm{c}}(1 + \frac{O_{\mathrm{i}}}{K_0})\right]} \tag{2}$$

$$A_{\mathrm{j}} = \left(\frac{J}{4}\right) \times \frac{\left(C_{\mathrm{i}} - \Gamma^*\right)}{\left(C_{\mathrm{i}} + 2\Gamma^*\right)} \tag{3}$$

where A_{m} is the hyperbolic minimum of Rubisco-limited (A_{c}) and RuBP regeneration limited photosynthesis (A_{j}). θ is a shape parameter set to 0.9999. V_{cmax} and J_{max} are the maximum carboxylation and electron transport rates (J_{max}), respectively; C_{i} and O_{i} are the intercellular concentrations of CO_2 and O_2, respectively; K_{c} and K_{o} are the Rubisco activity for CO_2 and O_2, respectively; and Γ^* is the CO_2 compensation point. The parameters V_{cmax} and J_{max} were fitted by R package *plantecophys* (Duursma, 2015).

2.3.3 Hydraulic traits

The hydraulic traits included stem embolism resistance, leaf drought tolerance (turgor loss parameters), and relative anisohydricity before drought treatment. In detail, stem embolism resistance (P_{50}) were derived from the stem vulnerability curves, which were measured by the air-dehydration method (Sperry *et al.*, 1988). For each species, 10 stems were dehydrated on a bench to obtain various degrees of drought. For each drought degree, xylem water potential was measured by a pressure chamber (SAP II

3115, SEC, US), and percentage loss of xylem hydraulic conductance (PLC) was measured by XYL'EM hydraulic conductance and embolism measurement system (INRA, France). For PLC measurement, 20~30 cm stems segments were cut under KCl solution (2 mM, Duan *et al.*, 2019). Among the five species, *C. gilva* and *C. sclerophylla* belong to family Fagaceae, and *N. chekiangense* and *P. chekiangensis* belong to family Lauraceae. The longest vessel length of both families was shorter than 20 cm (Jacobsen *et al.*, 2012). *S. superba* belongs to family Theaceae, whose vessel length was not available but the stem sample of a previous study on *S. superba* was 20-30 cm (Duan *et al.*, 2019). Therefore, the resulted vulnerability curves would not suffer the problem of shorter stems than vessel length. A reparameterized Weibull equation was used fit the vulnerability curve (Fig. 1; Ogle *et al.*, 2009):

$$PLC = 1-(1-\frac{X}{100})^{\left[\left(\frac{P}{P_X}\right)^{\frac{P_X S_X}{V}}\right]} \tag{4}$$

$$V = (X-100)\log(1-\frac{X}{100}) \tag{5}$$

where P_X is the xylem potential when PLC was X, and S_X is a shape parameter. The hydraulic safety margin (HSM) was quantified by two methods. One was the $\mathrm{HSM}_{\mathrm{min\text{-}88}}$, the difference between the minimum leaf water potential (Ψ_{min}) and P_{88}, and the other was $\mathrm{HSM}_{\mathrm{close\text{-}88}}$, the difference between the leaf water potential causing 90% stomatal closure (Ψ_{close}) and P_{88}. The Ψ_{min} was the minimum observed water potential of green leaves for plants able to recover. The Ψ_{close} was determined by constructing the relationship between stomatal conductance (g_{s}) and predawn leaf water potential (Ψ_{PD}) in plants under the drought treatment:

$$g_{\mathrm{s}} = b_1 e^{(-\Psi_{\mathrm{PD}}/b_2)^{b_3}} \tag{6}$$

Ψ_{close} is the Ψ_{PD} corresponding to the g_{s} being $0.1 \times b_1$.

Drought tolerance traits, π_{tlp} (leaf water potential at turgor loss point) and ε (modulus of elasticity) were derived from pressure-volume curves, which are the relationship between leaf water potential (Ψ) and relative water content. Pressure-volume curves were measured on five leaves for each species by the squeeze method (Schulte & Hinckley, 1985). The detailed measurement followed the online procedure in Prometheus Wiki (http://prometheuswiki.org/tiki-index.php?page=Leaf+pressure-volume+curve+parameters).

The degree of anisohydricity (σ) was calculated as the slope of the regression line between midday (Ψ_{MD}) and predawn leaf water potentials (Ψ_{PD}; Martinez-Vilalta *et al.*, 2014). This was achieved by a preliminary drought experiment on five individuals for each species. These individuals were located in the greenhouse with no water addition, and for every one to three days, the Ψ_{PD} and Ψ_{MD} of three randomly chosen individuals were measured. After removal of measurements with Ψ_{PD} near 0 (0-20% of data), the Ψ_{MD} was regressed against Ψ_{PD}, and the slope (σ) and intercept (Λ) were estimated (Martinez-Vilalta *et al.*, 2014).

2.4 Physiological and biomass measurements

During the drought period, spot measurements of leaf water potentials, photosynthesis, transpiration, stomatal conductance, leaf area and plant biomass were conducted every 3-5 days. These variables were measured every 1-2 days at the beginning but every 3-7 days during the late phase of the rewatering period. For each measurement point during the drought and rewatering periods, Ψ_{PD} (2:00 - 4:00 a.m.) and Ψ_{MD} (12:00 - 14:00 p.m.) were measured on three leaves (one per individual) for each species (n = 3). For plants that became partially defoliated, we chose leaves that had no obvious sign of wilting to determine the Ψ_{PD} and Ψ_{MD}. The Ψ_{MD} was not only affected by the soil water potential but also influenced by transpiration rate at the time of collection. To avoid the uncertainty induced by different weather conditions on different days, we used the Ψ_{PD} measurements to calculate stem PLC during the drought period based on the predetermined vulnerability curves. Although it was uncertain whether the vulnerability curves differed between drought and rewatering periods (Duan *et al.*, 2019), Hudson *et al.* (2018) found no response of vulnerability curve to water treatments in piñons and junipers. Therefore, we also calculated the stem PLC during the recovery period based on the vulnerability curves collected. After measurements of leaf water status, the plants were destructively sampled and separated into leaves, stems and roots. All the leaves were scanned and the total leaf area was determined by ImageJ (version 1.51s) software. All the samples were oven-dried and the biomass of leaves, stems and roots were measured. Net photosynthesis (A), transpiration (E) and stomatal conductance (g_s) were measured on three non-destructive individuals for each species and each treatment by using LI-6400 during 8:00 - 11:00 a.m. The temperature, relative humidity and light intensity were maintained around 25 °C, 60% and 1000 μ mol m^{-2} s^{-1}, respectively. The CO_2 concentration was set to ambient. To better illustrate the result, A, E and g_s in drought-rewatering groups were normalized by dividing them by the values of the control group.

2.5 Drought resistance and recovery

To quantify how A and E respond to drought, we adopted the framework in Hodgson *et al.* (2015), which used state change (*SC*) and return time (*RT*) to quantify the ability of a system to resist and recover from disturbance. For a specific day, the *SC* was $(1 - y_{\text{norm}}) \times 100\%$, where y_{norm} is the normalized A or E. The smaller the *SC*, the higher the resistance. For each recovery trajectory, y_{norm} was fitted against the days after rewatering (*DAR*) by an empirical equation:

$$y_{norm} = a_1 + a_2 \times \frac{DAR^{a_3}}{DAR^{a_3} + a_4} \tag{7}$$

where a_1 represents the y_{norm} before rewatering, (a_1 + a_2) determines the maximum extent that could recover to, and a_3 is a shape parameter accounting for the variation in shape of recovery trajectory among species. Based on Eqn 6, the return time to *x* percentage (RT_x) is:

$$RT_x = \sqrt[a_3]{\frac{a_4(x\% - a_1)}{a_1 + a_2 - x\%}} \tag{8}$$

We used $x = 20$, 50 and 80 to indicate the *A* and *E* recovery to low, medium and high levels, respectively. The smaller the RT_x, the faster recovery. To avoid over-parameterization in Eqn 6, linear interpolation was applied to calculate the *RT* if *A* or *E* recovered very quickly and exhibited a linear trajectory. The lower limit of *RT* was set to 0.5 because we rewatered the plants in the evening.

We also determined the survival time under drought according to the physiological measurements and rewatering experiments. The maximum survival time was defined as the drought days with all the leaves being brown or defoliated or no recovery was observed after rewatering. The minimum survival time was defined as the longest drought days after which at least 50% of leaves were green. The average survival time was calculated as the mean of the minimum and maximum.

2.7 Statistics

Differences in plant traits among five species were tested by one-way ANOVA or Kruskall-Wallis test. The regulation of plant traits on mortality, resistance and recovery were investigated by regressing the survival time, *SC* and *RT* against traits. The normality and homogeneity assumptions were checked by both plotting (Q-Q plot and scatter plot of model residuals for normality and homogeneity assumptions, respectively) and statistical methods (Shapiro-Wilk test and Fligner– Killeen test, respectively). For ANOVA, the traits clearly violating normality or homogeneity assumptions (Root:shoot ratio, SLA, LDMC, LA:BA, π_{tlp} and ε) were analyzed by Kruskall-Wallis test. For the traits derived from curve fitting and did not have real replications (P_{50}, P_{88}, Ψ_{close}, $\mathrm{HSM}_{\mathrm{close\text{-}88}}$, $\mathrm{HSM}_{\mathrm{min\text{-}88}}$), we used ANOVA from sufficient statistics for groups to conduct the multiple comparisons among species (*aov.sufficient* function in R package *HH*). For regressions, no clear violation of normality or homogeneity assumptions were found. All analyses were applied in R (version 3.5.1, R Core Team, 2018).

3 RESULTS

3.1 Environmental variables and extent of hydraulic failure

During the drought-rewatering experiment, the mean air temperature and relative humidity in the greenhouse was 32.1 ± 3.0 °C and 71.6 ± 7.2% (mean ± SD), respectively (Fig. 2a). The soil water content (SWC) in the control treatment was maintained at 21.1 ± 2.4% (Fig. 2b). The SWC in drought-rewatering treatments showed similar patterns among the five species. During the drought period, SWC dropped to ~5% after 20 days of withholding water. During the rewatering period, SWC rapidly recovered to the control levels within two days (Fig. 2b).

During the drought period, the extent of stem hydraulic failure, indicated by the percentage loss of hydraulic conductivity (PLC), increased with soil drying (Fig. 2c). After experiencing the same duration of drought, stem PLC of *C. sclerophylla* and *S. superba* was lower than that of the other species. Specifically, the lethal PLC threshold was 93, 91, 79, 78 and 64% for *C. gilva*, *C. sclerophylla*, *N. chekiangense*, *P.*

chekiangensis and *S. superba*, respectively ($F_{4,10} = 4.461$, $P = 0.025$, Fig. 2c).

3.2 Difference of plant traits among species

Morphologically, there were differences among the five species. Plant height and basal diameter were largest in *N. chekiangense*, whereas leaf size was largest in *P. chekiangensis* (Table 1). Differences in specific leaf area (SLA), leaf dry matter content (LDMC), and wood density were small (Table 1). No significant difference was found in root:shoot, leaf area:basal area ratio or photosynthetic traits (Table 1).

For the hydraulic traits, *C. sclerophylla* and *S. superba* were more resistant to embolism (i.e., more negative stem water potential causing 50% PLC, P_{50}), while *N. chekiangense* and *P. chekiangensis* were more drought tolerant with more negative turgor loss point (π_{tlp}) and larger modulus of elasticity (ε) (Table 1). However, the degree of anisohydricity (σ) was not significantly different among species (Table 1).

The 90% stomatal closure occurred later in *C. sclerophylla* and *S. superba* than in other species (Table 1; Appendix S1: Fig. S1b). The hydraulic safety margin calculated as the difference between the minimum leaf water potential and P_{88} (HSM_{min-88}) was largest in *P. chekiangensis*, followed by *S. superba*, *C. sclerophylla*, *N. chekiangense* and *C. gilva* (Table 1). The $HSM_{close-88}$, calculated as the difference between Ψ_{close} and P_{88}, was also largest in *P. chekiangensis* but lowest in *N. chekiangense* (Table 1).

3.3 Tree physiology and mortality under drought and rewatering periods

During the drought period, severe defoliation (> 50%) occurred after 14, 20, 20, 26 and 32 days of drought for *P. chekiangensis*, *C. gilva*, *N. chekiangense*, *S. superba* and *C. sclerophylla*, respectively (Appendix S1: Fig. S2). During the rewatering period, no new leaves developed in the defoliated plants. Both predawn (Ψ_{PD}) and midday leaf water potentials (Ψ_{MD}) decreased gradually during drought, and recovered to the pre-drought levels within three days after rewatering if there was no severe defoliation (Fig. 3). The recovery pattern of stem PLC was similar to that of leaf water potential (Appendix S1: Fig. S3).

The response and recovery patterns were similar among A, E, and g_s (Fig. 4; Appendix S1: Fig. S3). These variables could not fully recover when the drought ended after 8, 20, 26, 26 and 26 days for *P. chekiangensis*, *C. gilva*, *N. chekiangense*, *S. superba* and *C. sclerophylla*, respectively. The recovery velocity of A and E was much lower than those of SWC and leaf water status, especially when suffering severe droughts (Figs. 4c, f, I, l, o). For *C. gilva*, *C. sclerophylla* and *P. chekiangensis*, the leaf potential recovered to pre-drought level under severe drought but the A and E only exhibited partial recovery (Fig. 4).

The resistance (indicated by the state change, *SC*) and recovery (indicated by the return time, *RT*) of A and E differed among species and drought intensities (Appendix S1: Fig. S4). During the drought period, *P. chekiangensis* was the least resistant species, with the largest *SC* of both A and E, followed by *N. chekiangense*, *C. gilva*, *S. superba* and *C. sclerophylla*. Although the *SC* of E in *S. superba* was similar to that in *C. sclerophylla*, *S. superba* defoliated and died before *C. sclerophylla* (Appendix S1: Figs. S2 and S5).

P. chekiangensis was also the species that recovered slowest from drought, whose RT_{80} (return time to 80% of the control value) was much higher than other species in the R1 treatment (rewatering after 8 days of drought) and died after 20 days of drought (Figs. 5d and i). *N. chekiangense* and *C. gilva* both died after 26 days of drought (Fig. 5a, c, f and h). However, *C. gilva* had longer RT_{80} than *N. chekiangense* in R2 treatment (rewatering after 14 days of drought), and could not recover to 50% of the control value in the R3 treatment (rewatering after 20 days of drought). *S. superba* also died after 26 days of drought, but its *RT*s were slightly lower than *N. chekiangense*'s (Figs. 5e and j). *C. sclerophylla* was the most resilient species, which could recover to 50% of the control value in the R4 treatment (rewatering after 26 days of drought) and did not die until 32 days of drought (Figs. 5b and g).

3.4 Relationships between plant traits and tree resistance, recovery and mortality

Among all the morphological, photosynthetic and hydraulic traits, only the stem embolism resistance (P_{50}) could explain the variance in tree mortality, resistance and recovery among five species. The species that survived more days during drought had more negative P_{50} values ($r^2 = 0.89$, $P = 0.017$, Fig. 6a). With decreasing P_{50}, both the *SC* and *RT* decreased. The influence of stem P_{50} was alleviated for resistance but enhanced for recovery when the drought intensity increased (Fig. 7). Neither $\text{HSM}_{\text{min-88}}$ nor $\text{HSM}_{\text{close-88}}$ could explain the interspecific differences in tree mortality, *SC* or *RT* (Fig. 6b; Appendix S1: Figs. S6 and S7). In addition, no significant relationship was found between stem P_{50} and other traits (Appendix S1: Table S1).

4 DISCUSSION

4.1 Regulation of embolism resistance on tree mortality

In this study, species with greater stem embolism resistance (more negative P_{50}) survived longer under persistent drought (Fig. 6a), reflecting the important role of hydraulic failure to tree mortality. Some studies interpreted the influence of stem embolism resistance on tree death as the risk of trees to reach the lethal hydraulic failure (e.g., 88% percentage loss of conductance, PLC), which was usually indicated by hydraulic safety margin (HSM, Anderegg *et al.*, 2016). However, we found that neither the $\mathrm{HSM}_{\mathrm{min\text{-}88}}$ nor $\mathrm{HSM}_{\mathrm{close\text{-}88}}$ was correlated to the survival time or drought resilience among the five species (Fig. 6b; Appendix S1: Figs. S5-S7). This might be due to the lack of a general stem PLC threshold for tree death. For example, Adams *et al.* (2017) and McDowell *et al.* (2013) suggested that the lethal stem PLC was higher than 60%, whereas S. Li *et al.* (2015) showed that this value could be as high as 100%. In our study, the stem PLC threshold causing death varied from 64% to 93% (Fig. 2c). The observed lethal stem PLC might also be related to drought intensity and duration. In our experiment, the drought was rapid and severe, posing a direct impact on the stem hydraulics. If a more gradual and longer duration drought is conducted, the lethal stem PLC might be smaller than our observation in two situations: (1) the xylem embolism continuously develops even after the relief of drought stress (Gauthey *et al.*, 2022), or (2) the persistent drought depletes the non-structural carbohydrates, which is important to signaling of stomatal response, osmotic adjustments and embolism refilling (Klein *et al.*, 2018; Pou *et al.*, 2012).

Previous studies also showed other traits, such as anisohydricity and turgor loss point, could be important to tree death or drought resistance (Bartlett *et al.*, 2016; Kannenberg *et al.*, 2019). For instance, Martin-StPaul *et al.* (2017) showed that 90% stomatal closure generally occurred before 50% stem PLC, avoiding further water loss under drought. However, our results showed the opposite pattern (except for *C. sclerophylla*, Appendix S1: Fig. S1a). In this study, the more drought resistant species closed stomata later than the less resistant ones (Appendix S1: Fig. S1b). This evidence suggested that the reduced water loss due to stomatal closure may not be the primary factor causing the different drought resistance and mortality among the five species. Similarly, although leaf shedding may reduce water loss (Xu *et al.*, 2010), the species with earlier defoliation (*C.gilva*, *N. chekiangense* and *P. chekiangensis*) did not have higher drought resilience (Appendix S1: Figs. S1 and S2).

Turgor loss point (π_{tlp}) is another key trait that might be correlated to embolism resistance and tree mortality (Bartlett *et al.*, 2016; Zhu *et al.*, 2018). However, in this study, species with more negative π_{tlp} (*P. chekiangensis* and *N. chekiangense*) did not show higher drought resistance or longer survival time, instead of being highly sensitive to soil drying. Consistent with our results, another drought-rewatering experiment on three SEBF species in southern China suggested that the most drought resistant species had highest embolism resistance, but not the largest π_{tlp} (Duan *et al.*, 2019). More broadly, a global meta-analysis also showed a nonsignificant effect of π_{tlp} on tree mortality (Anderegg *et al.*, 2016). All these pieces of evidence suggest that the differential P_{50} among five species may actually reflect the passive response to drought, not the active mechanism coping with drought stress.

4.2 Regulation of embolism resistance on drought recovery of *A* and *E*

Previous studies have suggested that plant hydraulic traits, such as embolism resistance and isohydricity, may regulate the recovery of physiological rates (Brodribb *et al.*, 2010; Pou *et al.*, 2012; Peguero-Pina *et al.*, 2018). In our study, however, only the stem embolism resistance had significant effects on the recovery time of photosynthesis and transpiration among five species (Figs. 7c, d), highlighting the importance of hydraulic dysfunction in limiting the post-drought recovery (Urli *et al.*, 2013; Peguero-Pina *et al.*, 2018). The recovery of hydraulic function can be achieved via two mechanisms: embolism refilling and new xylem growth (Klein *et al.*, 2018). Embolism refilling occurs in very short time span (6-12 hours, Gauthey *et al.*, 2022), which might be important under mild and short droughts. When plants experience more severe drought, the xylem conduits might be damaged permanently. Thus, the recovery of plant water potential largely depend on the growth of new xylem, a process taking from weeks to months (Brodribb *et al.*, 2010; Duan *et al.*, 2019). In our study, the leaf water potential and apparent stem PLC recovered within 2-3 days after rewatering as long as there was no severe defoliation (Fig. 2; Appendix S1: Fig. S3), indicating that the rapid refilling might repair the xylem embolism. However, a recent study using microcomputed tomography to examine the xylem embolism in *Eucalyptus saligna* suggested that the stem water potential could fully recover in 24 hours despite the absence of embolism refilling or new xylem growth (Gauthey et al., 2022), suggesting further research is required to explicitly resolve the controversy debate on the mechanisms underlying the post-drought recovery of plant water status.

The recovery of photosynthesis and transpiration largely lagged behind that of leaf water status, taking 1-3 weeks to reach the normal levels (Fig. 4), probably due to the delayed recovery of stomatal conductance and biochemical components of photosynthesis (Li *et al.*, 2021). The reduction of stomatal conductance under drought can not only be induced by hydraulic factors, but also by non-hydraulic factors such as abscisic acid (ABA, Flexas *et al.*, 2009; Creek *et al.*, 2018). After rewatering, when the hydraulic system recovered, the previous accumulated ABA may still limit the stomatal conductance (McAdam & Brodribb, 2015), causing the slow recovery of photosynthesis and transpiration. The biochemical components (e.g., V_{cmax} and J_{max}) could be decreased by severe drought due to the inactivation of photosynthetical enzymes, thus limiting the recovery rate of photosynthesis (Flexas *et al.*, 2009; Li *et al.*, 2021). In addition, drought induced cell destruction may also delay the recovery of stomatal conductance (Miyashita *et al.*, 2005), and even cause permanent damage to the photosynthetic system (Trueba *et al.*, 2019), leading to incomplete recovery in tree physiology under severe droughts (Fig. 4).

4.3 Implications

The SEBF in China is a unique biome with high biodiversity and carbon sequestration (Yu *et al.*, 2014; Fan *et al.*, 2018), and experiences more frequent extreme droughts (Yuan *et al.*, 2016). It is difficult to directly apply our seedling results to mature trees (Hartmann *et al.*, 2018). However, the inferences on seedlings could still be valuable for the potential vulnerability of SEBFs, because forest restoration after destructive disturbances, such as extreme droughts and typhoon (Lin *et al.*, 2011), depends on the regeneration of tree seedlings. In this study, the little contribution of stomatal closure, leaf shedding and drought tolerance on the drought resilience in SEBF seedlings may be derived from the evolutionary background of these trees. As the SEBFs have historically suffered internal drought rarely in their evolutionary history, they may not have developed multiple drought strategies to increase their fitness. As a result, the SEBFs might be vulnerable to future co-ocurring climate extremes due to the failure of species regeneration. In fact, the difficulty of species regeneration caused by natural and human disturbances has already threatened the maintenance of SEBFs in southern China (Liu *et al.*, 2018; Chu *et al.*, 2019).

At the ecosystem scale, the forests in South America, Africa and Southeast Asia were more isohydric (i.e., rapid stomatal closure under drought) than SEBFs (Konings & Gentine, 2017), suggesting more effective drought strategy of these forests. Thus, SEBFs might be more vulnerable to future drought than the forests in these areas, probably because SEBFs have experienced less drought stresses. Bennett *et al.* (2021) also suggested that more severe historical drought stresses made the African tropical forests more drought-adapted and more resistant to El Niño-induced droughts than Amazonian and Southeast Asian forests. This conclusion was consistent with the observation that tree mortality rate greatly increased in Amazon forests but slightly decreased in Congo Basin (McDowell *et al.*, 2022). However, opposite evidence exists. Zhu *et al.* (2019) argued that SEBFs had less risk for hydraulic failure than tropical dry forests and Mediterranean-type woodlands because of the wider HSMs. As we had discussed, HSM may not be a reliable indicator of drought vulnerability for SEBFs. Nevertheless, considering the scarcity of studies that directly examine the drought mortality and recovery in SEBF, more drought-rewatering experiments are needed to investigate the actual vulnerability of SEBFs to future drought.

There was some uncertainties worth being highlighted and might be insightful for the future research. First, our drought treatment was very rapid and severe, which could be different from naturally-occurred drought. If the trees undergo more gradual and mild droughts, the stem hydraulic failure might occur more slowly, allowing other physiological processes (e.g., stomatal closure, leaf shedding and osmotic adjustments) take part in the process of tree death. In this case, other hydraulic traits could be related to drought resistance and resilience. Second, when the SWC is low, the soil water potential (SWP) could change dramatically even under the condition with the relatively unchanged SWC. Therefore, tracking the SWP during experiment could help to know better about the exact external drought stresses that plants experienced. Third, studies conducting repeated drought events showed that early exposure to water deficit can induce physiological or morphological changes that improved plant performance under later extreme droughts (Wang *et al.*, 2017). Studies on the multiple ecotypes or genotypes within the same species showed that the plasticity of physiological rates and hydraulic traits to drought can be adaptive (Challis *et al.*, 2022; Duan *et al.*, 2022). The existence of physiological acclimation and adaptation might help SEBFs to buffer the damage caused by severe drought. All these issues reflect the complicated mechanisms underlying drought response and recovery, which should be further studied for addressing the challenge of incorporating hydraulic dynamics into terrestrial biosphere models to better predict forest carbon and water cycling under future climate change (Medlyn *et al.*, 2016).

Acknowledgements

The authors thank the editor and two anonymous reviewers for their insightful comments and suggestions. This study was financially supported by the National Natural Science Foundation of China (Grant No. 31930072, 31600387), the National Key R&D Program of China (2017YFA06046). NGM was supported by the Department of Energy's Next Generation Ecosystem Experiment (NGEE)-Tropics project. We thank Weisong Cheng, Jing Gao, Nan Li, Ruiqiang Liu, Qin Luo, Jiawei Wang, Qing Wang, Guodong Zhang, Huimin Zhou and Guiyao Zhou for their great help to the experiment.

Conflict of Interest

The authors declare no conflict of interest.

Author Contributions

J.S. and X.Z. conceived the study. J.S., P.Z., D.Z., T.Y., and Z.L. conducted experiment. J.S. analyzed data. J.S. and X.Z. led the writing with contributions from all the authors.

Literature cited

Adams HD, Zeppel MJB, Anderegg WRL, Hartmann H, Landhäusser SM, Tissue DT, Huxman TE, Hudson PJ, Franz TE, Allen CD *et al.* 2017. A multi-species synthesis of physiological mechanisms in drought-induced tree mortality. *Nature Ecology and Evolution* 1: 1285–1291.

Anderegg WRL, Klein T, Bartlett M, Sack L, Pellegrini AFA, Choat B, Jansen S. 2016. Meta-analysis reveals that hydraulic traits explain cross-species patterns of drought-induced tree mortality across the globe. *Proceedings of the National Academy of Sciences* 113: 5024–5029.

Bartlett MK, Klein T, Jansen S, Choat B, Sack L. 2016. The correlations and sequence of plant stomatal, hydraulic, and wilting responses to drought. *Proceedings of the National Academy of Sciences* 113: 13098–13103.

Bennett AC, Dargie GC, Cuni-Sanchez A, Mukendi JT, Hubau W, Mukinzi JM, Phillips OL, Malhi Y, Sullivan MJP, Cooper DLM *et al.* 2021. Resistance of African tropical forests to an extreme climate anomaly. *Proceedings of the National Academy of Sciences* 118: e2003169118.

Brodribb TJ, Bowman DJMS, Nichols S, Delzon S, Burlett R. 2010. Xylem function and growth rate interact to determine recovery rates after exposure to extreme water deficit. *New Phytologist* 188: 533–542.

Challis A, Blackman, C, Ahrens C, Medlyn B, Rymer P, Tissue D. 2022. Adaptive plasticity in plant traits increases time to hydraulic failure under drought in a foundation tree. *Tree Physiology* 42: 708–721.

Chu X, Wang X, Zhang D, Wu X, Zhou Z. 2019. Responses of *Taxus chinensis* and *Phoebe chekiangensis* seedlings to controlled-release fertilizer in various formulations and application rates. *iForest - Biogeosciences and Forestry* 12:

254–261.

Creek D, Blackman CJ, Brodribb TJ, Choat B, Tissue DT. 2018. Coordination between leaf, stem, and root hydraulics and gas exchange in three arid-zone angiosperms during severe drought and recovery: Coordination between hydraulics and gas exchange during drought and recovery. *Plant, Cell & Environment* 41: 2869–2881.

Dai A. 2013. Increasing drought under global warming in observations and models. *Nature Climate Change* 3: 52–58.

de A. Lobo F, de Barros MP, Dalmagro HJ, Dalmolin ÂC, Pereira WE, de Souza ÉC, Vourlitis GL, Rodríguez Ortíz CE. 2013. Fitting net photosynthetic light-response curves with Microsoft Excel — a critical look at the models. *Photosynthetica* 51: 445–456.

Duan H, de Dios VR, Wang D, Zhao N, Huang G, Liu W, Wu J, Zhou S, Choat B, Tissue DT. 2022. Testing the limits of plant drought stress and subsequent recovery in four provenances of a widely distributed subtropical tree species. *Pllant, Cell and Environment* 45: 1187–1203.

Duan H, Li Y, Xu Y, Zhou S, Liu J, Tissue DT, Liu J. 2019. Contrasting drought sensitivity and post-drought resilience among three co-occurring tree species in subtropical China. *Agricultural and Forest Meteorology* 272–273: 55–68.

Duursma RA. 2015. Plantecophys - an R package for analysing and modelling leaf gas exchange data. *PLOS ONE* 10: e0143346.

Fan D, Huang J, Hu H, Sun Z, Cheng S, Kou Y, Zhang Z. 2018. Evolutionary Hotspots of Seed Plants in Subtropical China: A Comparison With Species Diversity Hotspots of Woody Seed Plants. *Frontiers in Genetics* 9: 333.

Flexas J, Barón M, Bota J, Ducruet J-M, Gallé A, Galmés J, Jiménez M, Pou A, Ribas-

Carbó M, Sajnani C *et al.* 2009. Photosynthesis limitations during water stress acclimation and recovery in the drought-adapted *Vitis* hybrid Richter-110 (*V. berlandierix* × *V. rupestris*). *Journal of Experimental Botany* 60: 2361–2377.

Garcia-Forner N, Adams HD, Sevanto S, Collins AD, Dickman LT, Hudson PJ, Zeppel MJB, Jenkins MW, Powers H, Martínez-Vilalta J *et al.* 2016. Responses of two semiarid conifer tree species to reduced precipitation and warming reveal new perspectives for stomatal regulation. *Plant, Cell and Environment* 39: 38–49.

Gauthey A, Peters JMR, Lòpez R, Carins-Murphy MR, Rodriguez-Dominguez CM, Tissue DT, Medlyn BE, Brodribb TJ, Choat B. 2022. Mechanisms of xylem hydraulic recovery after drought in *Eucalyptus saligna*. *Plant, Cell and Environment* 45: 1216–1228.

Hammond WM, Yu K, Wilson LA, Will RE, Anderegg WRL, Adams HD. 2019. Dead or dying? Quantifying the point of no return from hydraulic failure in drought - induced tree mortality. *New Phytologist* 223: 1834–1843.

Hartmann H, Moura CF, Anderegg WRL, Ruehr NK, Salmon Y, Allen CD, Arndt SK, Breshears DD, Davi H, Galbraith D *et al.* 2018. Research frontiers for improving our understanding of drought-induced tree and forest mortality. *New Phytologist* 218: 15–28.

Haughton N, Abramowitz G, De Kauwe MG, Pitman AJ. 2018. Does predictability of fluxes vary between FLUXNET sites? *Biogeosciences* 15: 4495–4513.

Hodgson D, McDonald JL, Hosken DJ. 2015. What do you mean, “resilient”? *Trends in Ecology and Evolution* 30: 503–506.

Hudson PJ, Limousin JM, Krofcheck DJ, Boutz AL, Pangle RE, Gehres N, McDowell NG, Pockman WT. 2018. Impacts of long-term precipitation manipulation on hydraulic architecture and xylem anatomy of piñon and juniper in Southwest

USA. *Plant, Cell and Environment* 41: 421–435.

Jacobsen AL, Pratt RB, Tobin MF, Hacke UG, Ewers FW. 2012. A global analysis of xylem vessel length in woody plants. *American Journal of Botany* 99: 1583–1591.

Kannenberg SA, Novick KA, Phillips RP. 2019. Anisohydric behavior linked to persistent hydraulic damage and delayed drought recovery across seven North American tree species. *New Phytologist* 222: 1862–1872.

Klein T, Zeppel MJB, Anderegg WRL, Bloemen J, De Kauwe MG, Hudson P, Ruehr NK, Powell TL, von Arx G, Nardini A. 2018. Xylem embolism refilling and resilience against drought-induced mortality in woody plants: processes and trade-offs. *Ecological Research* 33: 839–855.

Konings AG, Gentine P. 2017. Global variations in ecosystem-scale isohydricity. *Global Change Biology* 23: 891–905.

Kursar TA, Engelbrecht BM, Burke A, Tyree MT, EI Omari B, Giraldo JP. 2009. Tolerance to low leaf water status of tropical tree seedlings is related to drought performance and distribution. *Functional Ecology* 23: 93–102.

Levionnois S, Coste S, Nicolini E, Stahl C, Morel H, Heuret P. 2020. Scaling of petiole anatomies, mechanics and vasculatures with leaf size in the widespread Neotropical pioneer tree species *Cecropia obtusa* Trécul (Urticaceae). *Tree Physiology* 40: 245–258.

Li L, McCormack ML, Ma C, Kong D, Zhang Q, Chen X, Hui Z, Niinemets Ü, Guo D. 2015. Leaf economics and hydraulic traits are decoupled in five species-rich tropical-subtropical forests. *Ecology Letters* 18: 899–906.

Li S, Feifel M, Karimi Z, Schuldt B, Choat B, Jansen S. 2015. Leaf gas exchange performance and the lethal water potential of five European species during drought. *Tree Physiology* 36: 179–192.

Li W, Tian X, Sheng H, Liu Y, Zhang R. 2019. Effects of drought stress and re-watering on photosynthesis and root growth of *Phoebe chekiangensis*. *Ecological Science* 38: 182–188.

Li X, Bao J, Wang J, Blackman C, Tissue D. 2021. Antecedent drought condition affects responses of plant physiology and growth to drought and post-drought recovery. *Frontiers in Forests and Global Change* 4: 704470.

Lin T-C, Hamburg SP, Lin K-C, Wang L-J, Chang C-T, Hsia Y-J, Vadeboncoeur MA, McMullen GMM, Liu C-P. 2011. Typhoon disturbance and forest dynamics: lessons from a northwest pacific subtropical forest. *Ecosystems* 14: 127–143.

Liu B, Liu Q, Daryanto S, Guo S, Huang Z, Wang Z, Wang L, Ma X. 2018. Responses of *Chinese fir* and *Schima superba* seedlings to light gradients: implications for the restoration of mixed broadleaf-conifer forests from Chinese fir monocultures. *Forest Ecology and Management* 419–420: 51–57.

Martínez-Vilalta J, Poyatos R, Aguadé D, Retana J, Mencuccini M. 2014. A new look at water transport regulation in plants. *New Phytologist* 204: 105–115.

Martin-StPaul N, Delzon S, Cochard, H. 2017. Plant resistance to drought depends on timely stomatal closure. *Ecology Letters* 20: 1437–1447.

McAdam SAM, Brodribb TJ. 2015. The evolution of mechanisms driving the stomatal response to vapor pressure deficit. *Plant Physiology* 167: 833–843.

McDowell NG, Fisher RA, Xu C, Domec JC, Hölttä T, Mackay DS, Sperry JS, Boutz A, Kickman L, Gehres N *et al.* 2013. Evaluating theories of drought-induced vegetation mortality using a multimodel–experiment framework. *New Phytologist* 200: 304–321.

McDowell NG, Sapes G, Pivovaroff A, Adams HD, Allen CD, Anderegg WRL, Arend

M, Breshears DD, Brodribb T, Choat B *et al.* 2022. Mechanisms of woody-plant mortality under rising drought, CO_2 and vapour pressure deficit. *Nature Reviews Earth & Environment* 3: 294–308.

Medlyn BE, De Kauwe MG, Duursma RA. 2016. New developments in the effort to model ecosystems under water stress. *New Phytologist* 212: 5–7.

Meinzer FC, McCulloh KA. 2013. Xylem recovery from drought-induced embolism: where is the hydraulic point of no return? *Tree Physiology* 33: 331–334.

Miyashita K, Tanakamaru S, Maitani T, Kimura K. 2005. Recovery responses of photosynthesis, transpiration, and stomatal conductance in kidney bean following drought stress. *Environmental and Experimental Botany* 53: 205–214.

Mursinna AR, McCormick E, Van Horn K, Sartin L, Matheny AM. 2018. Plant hydraulic trait covariation: a global meta-analysis to reduce degrees of freedom in trait-based hydrologic models. *Forests* 9: 446.

Ogle K, Barber JJ, Willson C, Thompson B. 2009. Hierarchical statistical modeling of xylem vulnerability to cavitation. *New Phytologist* 182: 541–554.

Pan Y, Birdsey RA, Phillips OL, Jackson RB. 2013. The structure, distribution, and biomass of the world's forests. *Annual Review of Ecology, Evolution, and Systematics* 44: 593–622.

Peguero-Pina J, Mendoza-Herrer Ó, Gil-Pelegrín E, Sancho-Knapik D. 2018. Cavitation limits the recovery of gas exchange after severe drought stress in holm oak (*Quercus ilex* L.). *Forests* 9: 443.

Pérez-Harguindeguy N, Díaz S, Garnier E, Lavorel S, Poorter H, Jaureguiberry P, Bret-Harte MS, Cornwell WK, Craine JM, Curvich DE *et al.* 2013. New handbook for standardised measurement of plant functional traits worldwide. *Australian Journal of Botany* 61: 167–234.

Pou A, Medrano H, Tomàs M, Martorell S, Ribas-Carbó M, Flexas J. 2012. Anisohydric behaviour in grapevines results in better performance under moderate water stress and recovery than isohydric behaviour. *Plant and Soil* 359: 335–349.

R Core Team. 2018. R: A language and environment for statistical computing. R Foundation for Statistical Computing, Vienna, Austria. https://www.R-project.org/

Roman DT, Novick KA, Brzostek ER, Dragoni D, Rahman F, Phillips RP. 2015. The role of isohydric and anisohydric species in determining ecosystem-scale response to severe drought. *Oecologia* 179: 641–654.

Schulte PJ, Hinckley TM. 1985. A Comparison of Pressure-Volume Curve Data Analysis Techniques. *Journal of Experimental Botany* 36: 1590–1602.

Shao, J. 2022. Dataset of drought-rewatering experiment on five subtropical tree species. Figshare, data set. https://doi.org/10.6084/m9.figshare.20326380.v1

Sperry JS, Donnelly JR, Tyree MT. 1988. A method for measuring hydraulic conductivity and embolism in xylem. *Plant, Cell and Environment* 11: 35–40.

Trueba S, Pan R, Scoffoni C, John GP, Davis SD, Sack L. 2019. Thresholds for leaf damage due to dehydration: declines of hydraulic function, stomatal conductance and cellular integrity precede those for photochemistry. *New Phytologist* 223: 134–149.

Urli M, Porte AJ, Cochard H, Guengant Y, Burlett R, Delzon S. 2013. Xylem embolism threshold for catastrophic hydraulic failure in angiosperm trees. *Tree Physiology* 33: 672–683.

Vargas R, Sonnentag O, Abramowitz G, Carrara A, Chen JM, Ciais P, Correia A, Keenan TF, Kobayashi H, Ourcival J-M, *et al.* 2013. Drought influences the accuracy of simulated ecosystem fluxes: a model-data meta-analysis for

Mediterranean oak woodlands. *Ecosystems* 16: 749–764.

Wang S, Callaway RM, Zhou D-W, Weiner J. 2017. Experience of inundation or drought alters the responses of plants to subsequent water conditions. *Journal of Ecology* 105: 176–187.

Xu Z, Zhou G, Shimizu H. 2010. Plant responses to drought and rewatering. *Plant Signaling and Behavior* 5: 649–654.

Yan E-R, Wang X-H, Huang J-J. 2006. Shifts in plant nutrient use strategies under secondary forest succession. *Plant and Soil* 289: 187–197.

Yu G, Chen Z, Piao S, Peng C, Ciais P, Wang Q, Li X, Zhu X. 2014. High carbon dioxide uptake by subtropical forest ecosystems in the East Asian monsoon region. *Proceedings of the National Academy of Sciences* 111: 4910–4915.

Yuan W, Cai W, Chen Y, Liu S, Dong W, Zhang H, Yu G, Chen Z, He H, Guo W et *al.* 2016. Severe summer heatwave and drought strongly reduced carbon uptake in Southern China. *Scientific Reports* 6: 18813.

Zhu S-D, Chen Y-J, Ye Q, He P-C, Liu H, Li R-H, Fu P-L, Jiang G-F, Cao K-F. 2018. Leaf turgor loss point is correlated with drought tolerance and leaf carbon economics traits. *Tree Physiology* 38: 658–663.

Zhu S-D, Li R-H, He P-C, Siddiq Z, Cao K-F, Ye Q. 2019. Large branch and leaf hydraulic safety margins in subtropical evergreen broadleaved forest. *Tree Physiology* 39: 1405–1415.

Table 1 The morphological, photosynthetic and hydraulic traits of the five species.

Trait	*C. gilva*	*C. sclerophylla*	*N. chekiangense*	*P. chekiangensis*	*S. superba*	*n*
Porous	diffuse	ring	diffuse	diffuse	diffuse	
Height (cm)	67.81±0.58^{B}	45.74±0.44^{D}	87.80±0.71^{A}	58.58±0.34^{C}	60.12±0.54^{C}	249
Diameter (mm)	7.24±0.08^{B}	5.40±0.06^{E}	8.56±0.09^{A}	6.90±0.05^{C}	6.21±0.06^{D}	249
Root:shoot	0.75±0.12	0.51±0.03	0.49±0.07	0.55±0.06	0.48±0.05	5
Leaf size (cm^{2})	8.39±0.58^{C}	13.76±0.39^{B}	13.43±0.33^{B}	20.84±0.39^{A}	14.67±0.80^{B}	25
SLA (cm^{2} g^{-1})	124±4^{A}	114±8^{AB}	103±3^{B}	106±4^{B}	113±6^{AB}	25
LDMC	0.42±0.02^{AB}	0.43±0.00^{A}	0.43±0.02^{AB}	0.41±0.01^{AB}	0.36±0.02^{B}	25
Wood density (g cm^{-3})	0.56±0.03^{AB}	0.55±0.02^{AB}	0.48±0.03^{B}	0.51±0.01^{AB}	0.61±0.02^{A}	5
LA:BA	2094±453	1665±261	1850±349	2886±202	2523±279	5
A_{max} (μ mol m^{-2} s^{-1})	12.67±1.08	15.43±1.70	12.70±1.09	14.17±0.39	13.40±1.06	5
K_{m} (μ mol m^{-2} s^{-1})	145±21	198±32	155±21	170±16	197±26	5
Rd (μ mol m^{-2} s^{-1})	1.14±0.25	1.27±0.09	1.23±0.25	1.15±0.26	1.05±0.15	5
LCP (μ mol m^{-2} s^{-1})	14±3	17±2	16±2	14±1	17±4	5
α	0.072±0.005	0.070±0.011	0.072±0.012	0.080±0.008	0.081±0.007	5
V_{cmax} (μ mol m^{-2} s^{-1})	41.99±4.78	45.11±4.09	37.04±4.15	39.07±2.01	32.75±5.41	5
J_{max} (μ mol m^{-2} s^{-1})	81.03±9.45	96.81±18.73	86.88±21.07	82.91±9.58	71.20±9.73	5
J_{max}: V_{cmax}	1.96±0.22	2.10±0.28	2.28±0.29	2.13±0.22	2.22±0.19	5
P_{50} (MPa)	-0.91±0.08^{A}	-2.46±0.11^{C}	-1.33±0.07^{B}	-0.67±0.13^{A}	-1.92±0.12^{C}	10
P_{88} (MPa)	-2.77±0.299^{AB}	-3.23±0.19^{AB}	-2.27±0.09^{A}	-6.80±0.70^{C}	-3.94±0.36^{B}	10
Ψ_{close} (MPa)	-1.80±0.19	-1.80±0.17	-2.50±0.14	-3.13±0.68	-2.29±0.21	3
Ψ_{min} (MPa)	-3.94±0.24	-3.53±0.22	-3.50±0.25	-3.50±0.35	-2.85±0.24	3
$HSM_{close-88}$ (MPa)	0.97±0.10^{BC}	1.43±0.14 ^{BC}	-0.23±0.01^{C}	3.67±0.80^{A}	1.65±0.15^{B}	3
HSM_{min-88} (MPa)	-1.32±0.08^{D}	-0.30±0.02^{C}	-1.23±0.09^{D}	3.30±0.33^{A}	1.09±0.09^{B}	3
σ	0.64±0.13	0.54±0.07	0.81±0.10	0.71±0.11	0.69±0.06	5
Λ (MPa)	-1.42±0.25^{CD}	-1.69±0.15^{D}	-1.10±0.14^{B}	-1.37±0.18^{C}	-1.00±0.13^{A}	5
π_{tlp} (MPa)	-1.98±0.09^{A}	-2.20±0.03^{A}	-2.60±0.04^{B}	-2.50±0.04^{B}	-1.98±0.14^{A}	5
ε (MPa)	8.94±2.21^{B}	11.97±1.44^{AB}	24.15±1.87^{A}	17.94±3.85^{AB}	10.65±0.51^{B}	5
Survival time (days)	21.5±1.5	29±3	21.5±1.5	15.5±1.5	24.5±1.5	

Note: The values for survival time is mean±0.5×range and mean±se for other traits. The comparison among species was conducted by Kruskall-Wallis test for Root:Shoot, SLA, LDMC, LA:BA, π_{tlp} and ε, and by one-way ANOVA for other traits. No statistical test was conducted for survival time because it represents the ranges. Samples size (*n*) for A_{max}, K_m, Rd, LCP, α of *S. superba* is 4. Sample size for V_{cmax}, J_{max}, and J_{max}: V_{cmax} of *C. gilva*, *P. chekiangensis* and *S. superba* is 4 whereas that of *N. chekiangense* is 3. SLA: specific leaf area; LDMC, leaf dry matter content; LA:BA, the ratio between leaf area and basal area; A_{max}, light-saturated photosynthetic rate; K_m, Michaelis constant for light response curve; Rd, dark respiration; LCP, light compensation point; α, quantum efficiency; V_{cmax}, maximum rate of carboxylation; J_{max}, maximum rate of electron transport; P_{50}, xylem water potential at 50% loss of hydraulic conductivity; P_{88}, xylem water potential at 88% loss of hydraulic conductivity; Ψ_{close}, leaf water potential causing 90% stomatal closure; Ψ_{min}, minimum leaf water potential; $HSM_{close\text{-}88}$, hydraulic safety margin from Ψ_{close} to P_{88}; $HSM_{min\text{-}88}$, hydraulic safety margin from Ψ_{min} to P_{88}; σ, isohydricity; Λ, leaf water potential at soil potential = 0; π_{tlp}, turgor loss point; ε, bulk modulus of elasticity.

Figure captions

Figure 1. Stem vulnerability curves of the five species. The horizontal dash lines represent 50 and 88 percentage loss of hydraulic conductance. Cg, *C. gilva*; Cs, *C. sclerophylla*; Nc, *N. chekiangense*; Pc, *P. chekiangensis*; Ss, *S. superba*.

Figure 2. Dynamics in air temperature (Ta), relative humidity (RH), soil water content (SWC), and percentage loss of hydraulic conductivity (PLC) during the experiments. The red and green arrows in (a) indicate the onsets of drought and rewetting treatments, respectively. The colored crosses in (c) represent the average survival days of each species. CK, control; Dr, drought treatment; R1-R7, rewetting after 8, 14, 20, 26, 32, 38 and 44 days' drought, respectively. Cg, *C. gilva*; Cs, *C. sclerophylla*; Nc, *N. chekiangense*; Pc, *P. chekiangensis*; Ss, *S. superba*.

Figure 3. The response and recovery of predawn (a, c, e, g, i) and midday leaf water potentials (b, d, f, h, j) to persistent drought and rewetting for the five species. Dr, drought treatment; R1, rewetting after 8 days' drought; R2, rewetting after 14 days' drought; R3, rewetting after 20 days' drought; R4, rewetting after 26 days' drought.

Figure 4. The response and recovery of photosynthesis rate (A, a, d, g, j, m), transpiration rate (E, b, e, h, k, n) to persistent drought and rewetting, and comparisons of the recovery of leaf water potential, A and E. Note that the A amd E were normalized for the convenience of comparisons. The third column showed recovery from the most severe drought before tree death. The grey horizontal lines represent the A_{norm} and E_{norm} of plants in CK groups. Dr, drought treatment; R1, rewetting after 8 days' drought; R2, rewetting after 14 days' drought; R3, rewetting after 20 days' drought; R4, rewetting after 26 days' drought.

Figure 5. The 20%, 50% and 80% return time (*RT*) of photosynthesis (a - e) and transpiration (f - j) in five species during the rewatering period. The shorter the *RT*,

the higher the resilience. The horizontal grey line indicates the plant is not able to return to the specific percentage of control. The black crosses indicate plant death. R1, rewetting after 8 days' drought; R2, rewetting after 14 days' drought; R3, rewetting after 20 days' drought; R4, rewetting after 26 days' drought.

Figure 6. Influences of P_{50} and $\mathrm{HSM}_{\mathrm{min\text{-}88}}$ on the survival time. Cg, *C. gilva*; Cs, *C. sclerophylla*; Nc, *N. chekiangense*; Pc, *P. chekiangensis*; Ss, *S. superba*.

Figure 7. Influences of P_{50} on the resistance (indicated by the state change, *SC*) and recovery (indicated by the 50% return time, RT_{50}) of photosynthesis (*A*) and transpiration (*E*) to persistent drought and rewatering, respectively. The *SC* was the values at DOY 214, 220, 226, and 232, respectively. Cg, *C. gilva*; Cs, *C. sclerophylla*; Nc, *N. chekiangense*; Pc, *P. chekiangensis*; Ss, *S. superba*. R1, rewetting after 8 days' drought; R2, rewetting after 14 days' drought; R3, rewetting after 20 days' drought; R4, rewetting after 26 days' drought.

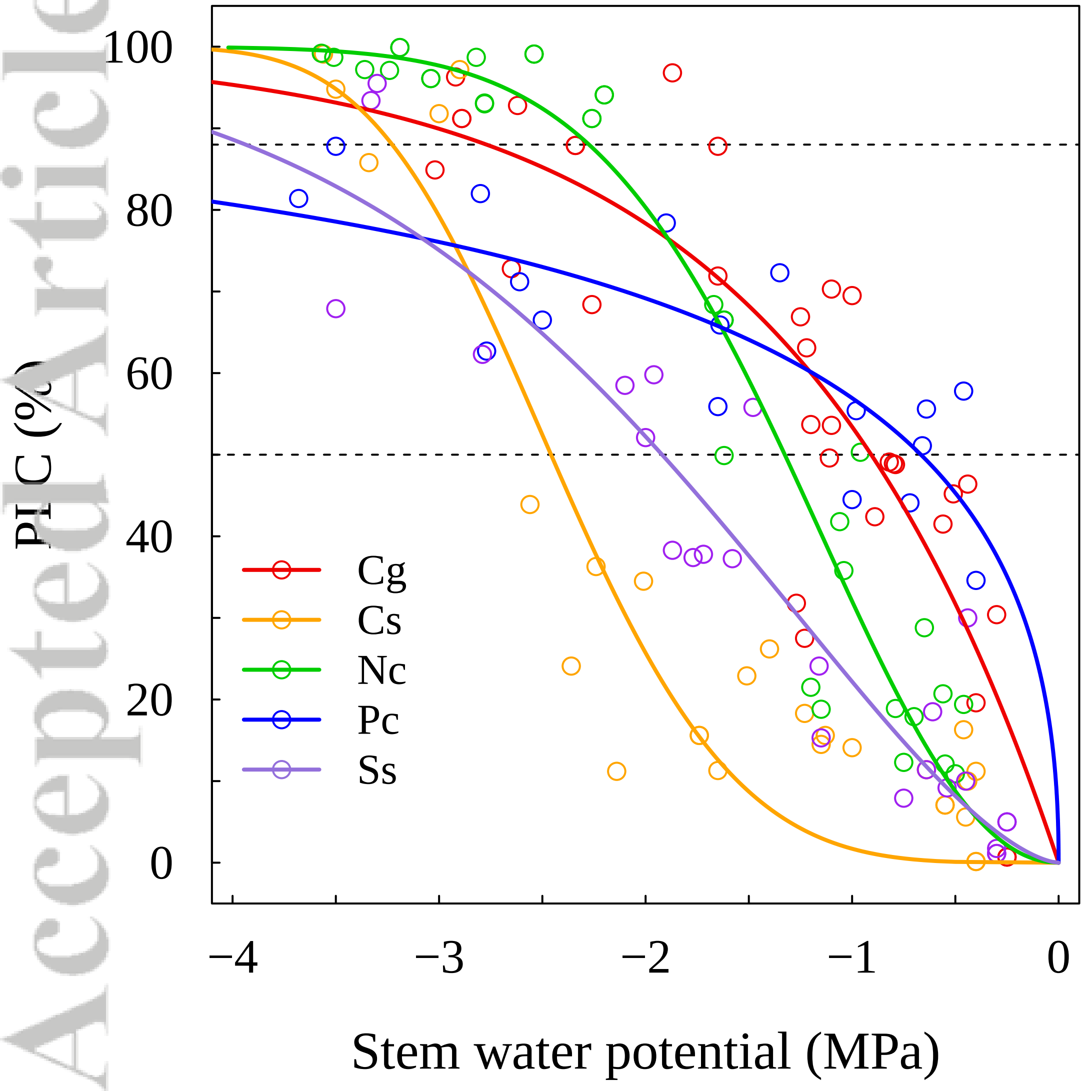
100
80
60
40
20
0
PLC (%)
−4
−3
−2
−1
0
Stem water potential (MPa)
Cg
Cs
Nc
Pc
Ss

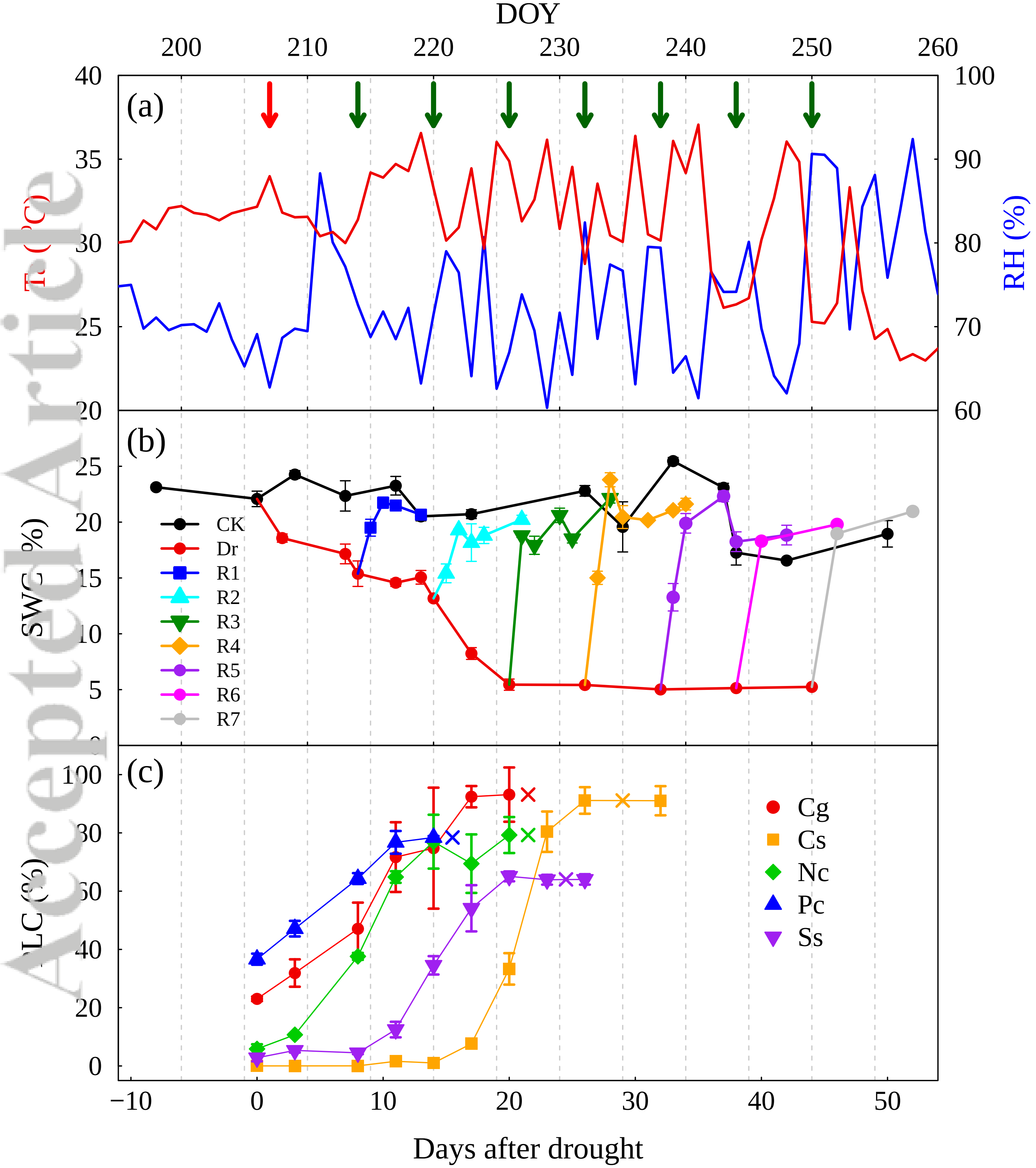
DOY
200
210
220
230
240
250
260
(a)
40
35
30
25
20
100
90
80
70
60
Ta (°C)
RH (%)
(b)
25
20
15
10
5
0
SWC (%)
CK
Dr
R1
R2
R3
R4
R5
R6
R7
(c)
100
80
60
40
20
0
PLC (%)
Cg
Cs
Nc
Pc
Ss
−10
0
10
20
30
40
50
Days after drought

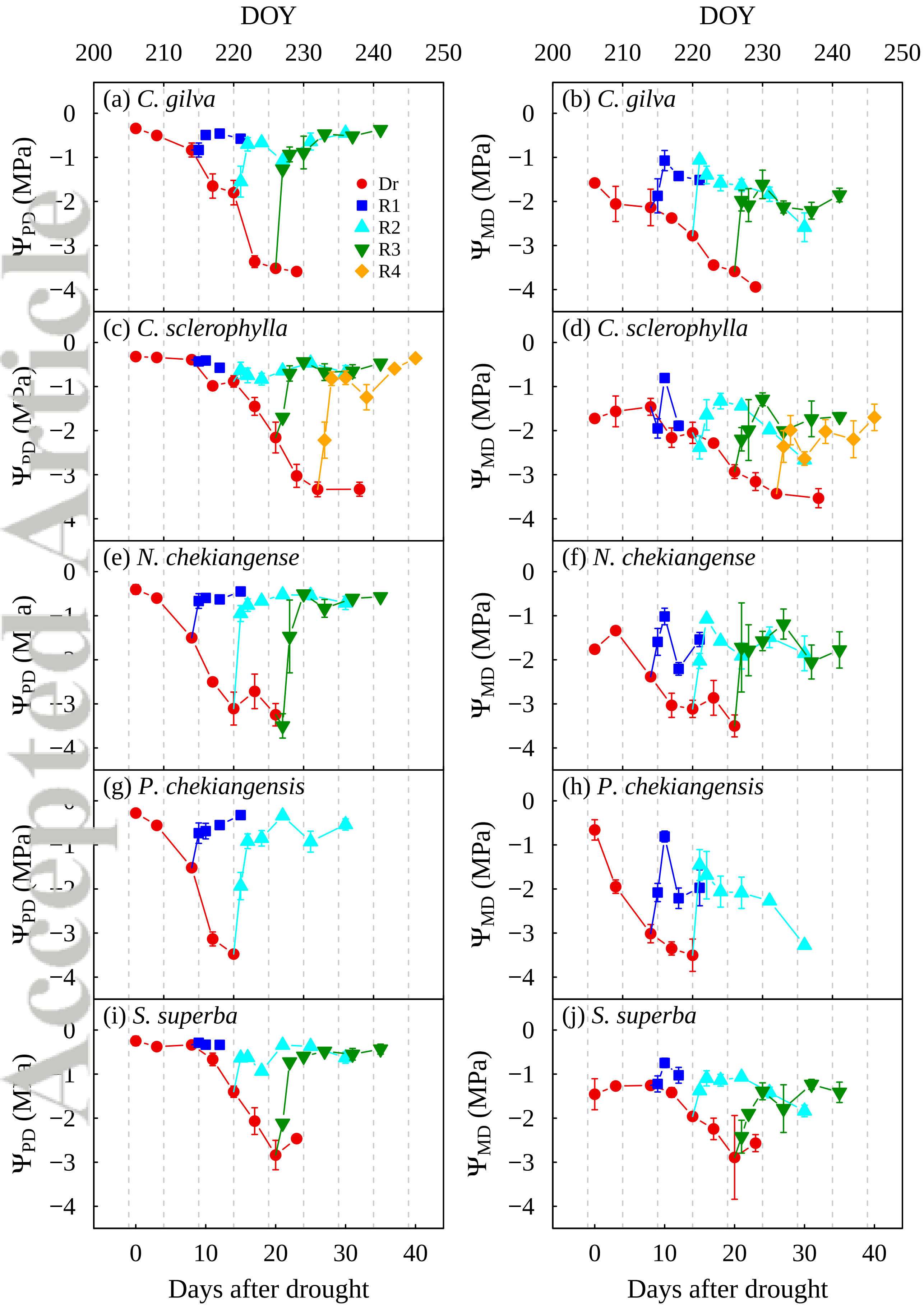
DOY
200
210
220
230
240
250
DOY
200
210
220
230
240
250
(a) *C. gilva*
(b) *C. gilva*
(c) *C. sclerophylla*
(d) *C. sclerophylla*
(e) *N. chekiangense*
(f) *N. chekiangense*
(g) *P. chekiangensis*
(h) *P. chekiangensis*
(i) *S. superba*
(j) *S. superba*
Dr
R1
R2
R3
R4
Ψ_{PD} (MPa)
Ψ_{MD} (MPa)
0
−1
−2
−3
−4
0
10
20
30
40
Days after drought
Days after drought

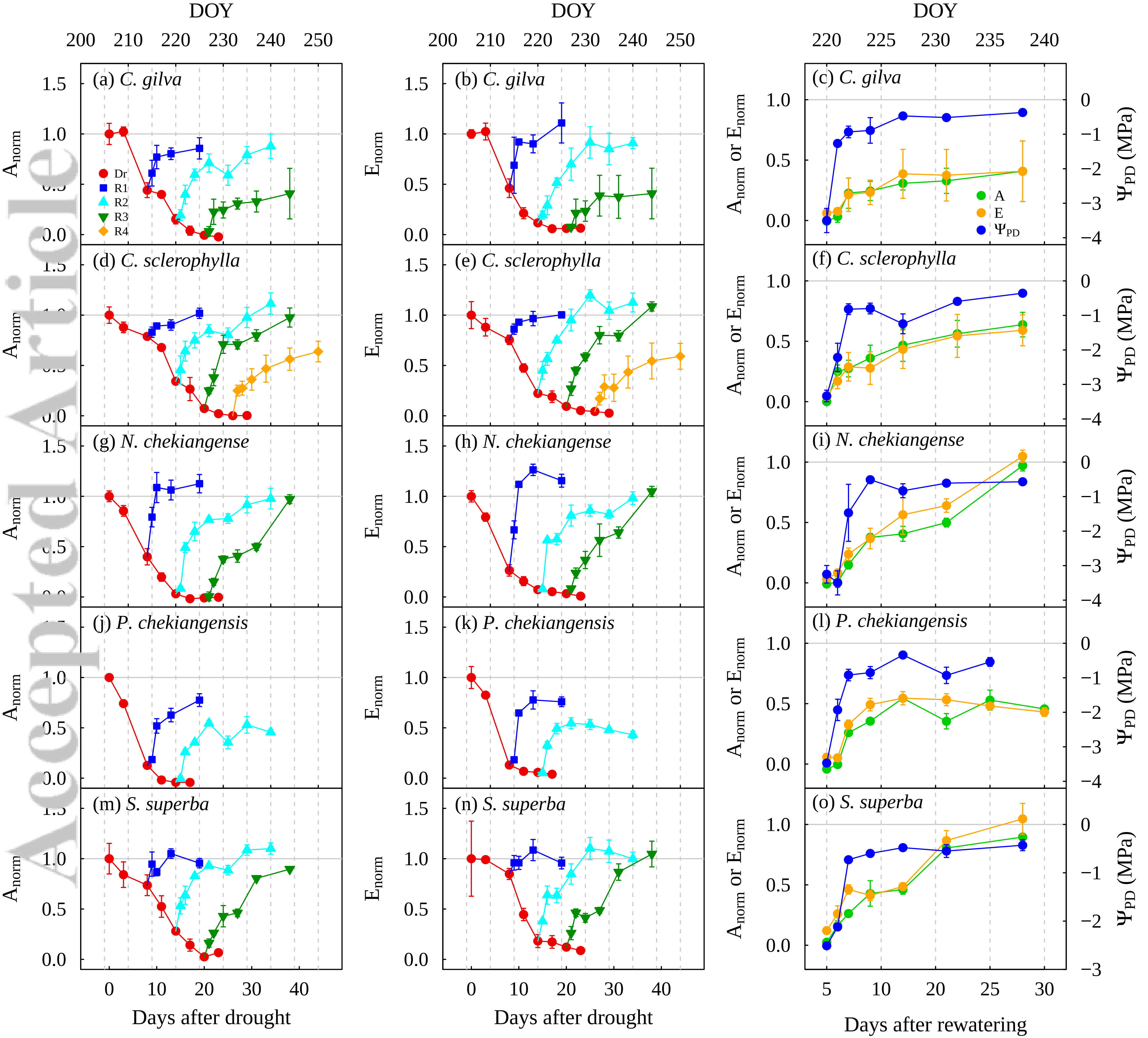
DOY
200
210
220
230
240
250
DOY
200
210
220
230
240
250
DOY
220
225
230
235
240
(a) C. gilva
(b) C. gilva
(c) C. gilva
(d) C. sclerophylla
(e) C. sclerophylla
(f) C. sclerophylla
(g) N. chekiangense
(h) N. chekiangense
(i) N. chekiangense
(j) P. chekiangensis
(k) P. chekiangensis
(l) P. chekiangensis
(m) S. superba
(n) S. superba
(o) S. superba
Dr
R1
R2
R3
R4
A
E
Ψ_PD
A_norm
E_norm
A_norm or E_norm
Ψ_PD (MPa)
0.0
0.5
1.0
1.5
0
−1
−2
−3
−4
0
10
20
30
40
5
10
20
25
30
Days after drought
Days after drought
Days after rewatering

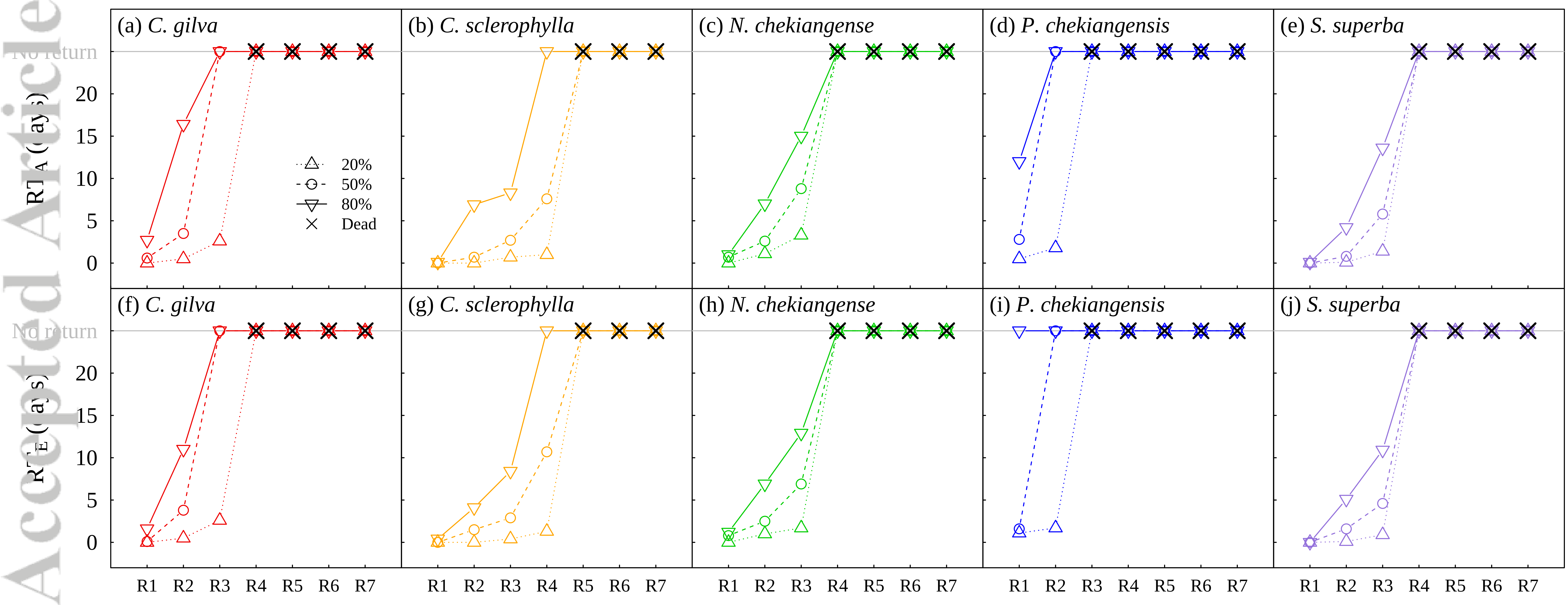
(a) C. gilva
(b) C. sclerophylla
(c) N. chekiangense
(d) P. chekiangensis
(e) S. superba
(f) C. gilva
(g) C. sclerophylla
(h) N. chekiangense
(i) P. chekiangensis
(j) S. superba
No return
No return
RT$_A$ (days)
RT$_E$ (days)
0
5
10
15
20
20%
50%
80%
Dead
R1
R2
R3
R4
R5
R6
R7

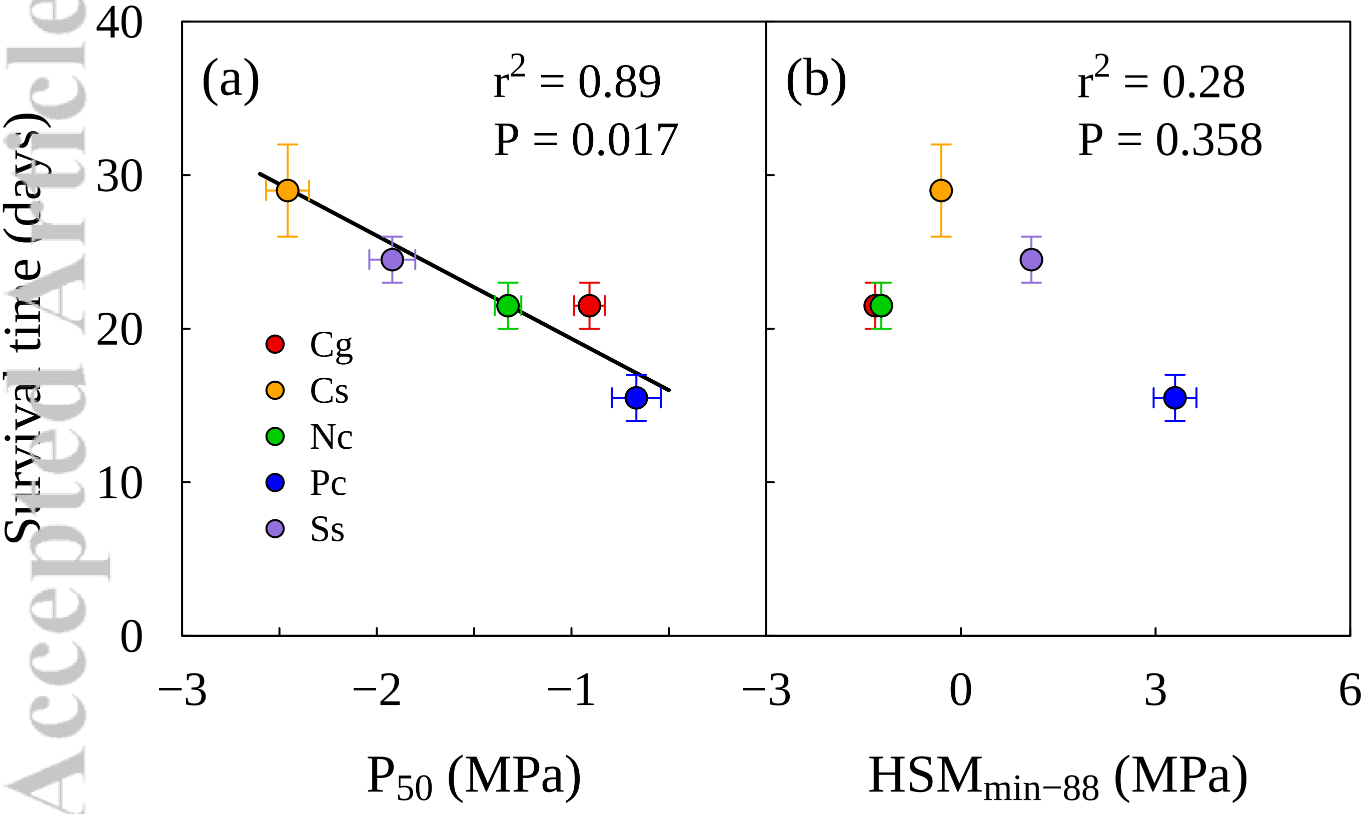
Survival time (days)
0
10
20
30
40
(a)
$r^2 = 0.89$
$P = 0.017$
● Cg
● Cs
● Nc
● Pc
● Ss
−3
−2
−1
P_{50} (MPa)
(b)
$r^2 = 0.28$
$P = 0.358$
−3
0
3
6
HSM_{min-88} (MPa)

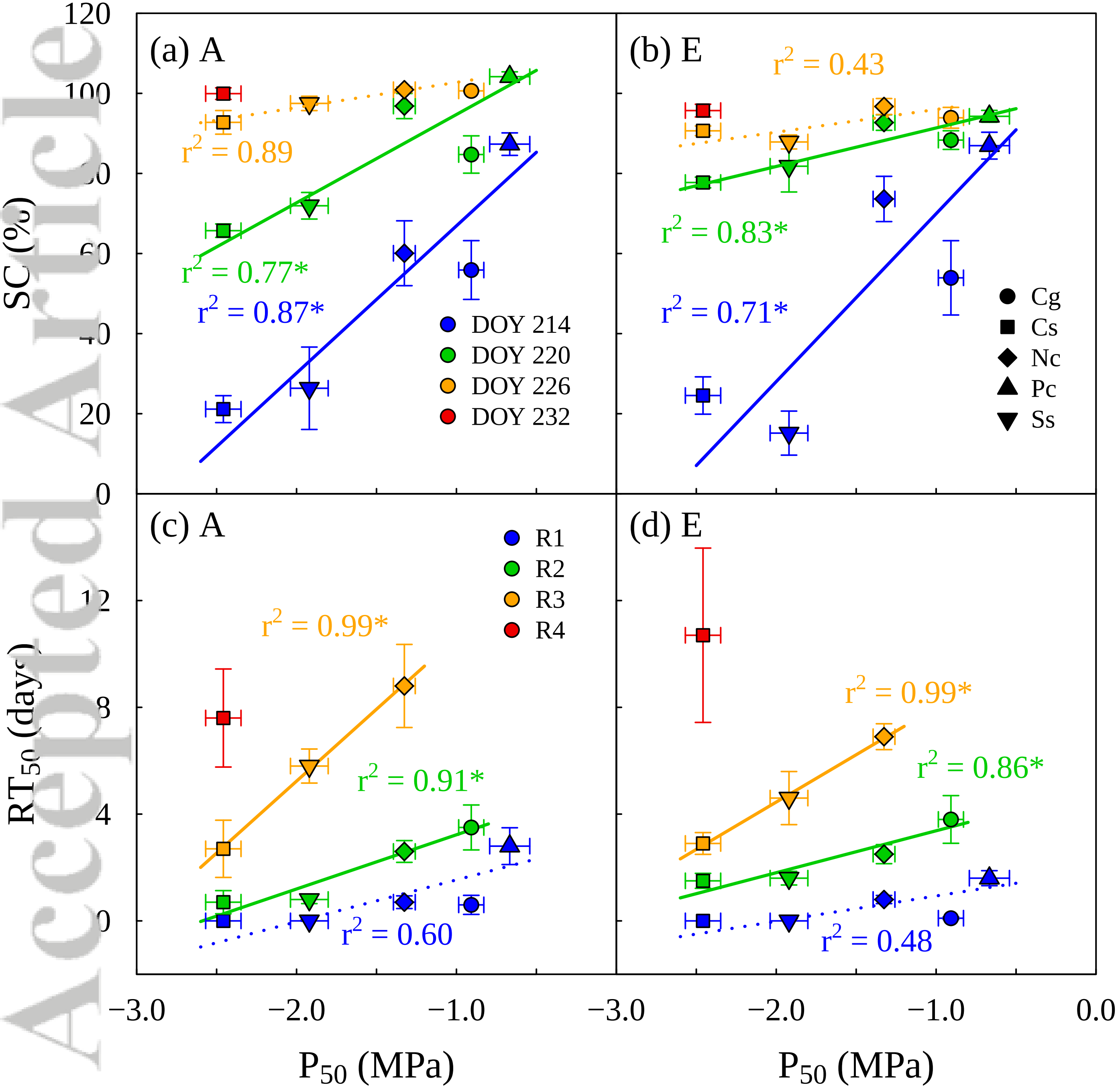
(a) A
(b) E
(c) A
(d) E
SC (%)
RT$_{50}$ (days)
P$_{50}$ (MPa)
P$_{50}$ (MPa)
0
20
40
60
80
100
120
0
4
8
12
−3.0
−2.0
−1.0
−3.0
−2.0
−1.0
0.0
r^2 = 0.89
r^2 = 0.77*
r^2 = 0.87*
r^2 = 0.43
r^2 = 0.83*
r^2 = 0.71*
r^2 = 0.99*
r^2 = 0.91*
r^2 = 0.60
r^2 = 0.99*
r^2 = 0.86*
r^2 = 0.48
DOY 214
DOY 220
DOY 226
DOY 232
Cg
Cs
Nc
Pc
Ss
R1
R2
R3
R4